Research
Engineering Management—Article

Unmanned Aerial Vehicle Inspection Routing and Scheduling for Engineering Management

Lu Zhen [a], Zhiyuan Yang [a], Gilbert Laporte [b,c], Wen Yi [d,*], Tianyi Fan [a]

[a] School of Management, Shanghai University, Shanghai 200444, China
[b] Department of Decision Sciences, HEC Montréal, Montréal PQ H3T 2A7, Canada
[c] School of Management, University of Bath, Bath BA2 7AY, UK
[d] Department of Building and Real Estate, The Hong Kong Polytechnic University, Hong Kong 999077, China

ABSTRACT

Technological advancements in unmanned aerial vehicles (UAVs) have revolutionized various industries, enabling the widespread adoption of UAV-based solutions. In engineering management, UAV-based inspection has emerged as a highly efficient method for identifying hidden risks in high-risk construction environments, surpassing traditional inspection techniques. Building on this foundation, this paper delves into the optimization of UAV inspection routing and scheduling, addressing the complexity introduced by factors such as no-fly zones, monitoring-interval time windows, and multiple monitoring rounds. To tackle this challenging problem, we propose a mixed-integer linear programming (MILP) model that optimizes inspection task assignments, monitoring sequence schedules, and charging decisions. The comprehensive consideration of these factors differentiates our problem from conventional vehicle routing problem (VRP), leading to a mathematically intractable model for commercial solvers in the case of large-scale instances. To overcome this limitation, we design a tailored variable neighborhood search (VNS) metaheuristic, customizing the algorithm to efficiently solve our model. Extensive numerical experiments are conducted to validate the efficacy of our proposed algorithm, demonstrating its scalability for both large-scale and real-scale instances. Sensitivity experiments and a case study based on an actual engineering project are also conducted, providing valuable insights for engineering managers to enhance inspection work efficiency.

© 2024 Published by Elsevier Ltd. on behalf of Chinese Academy of Engineering. This is an open access article under the CC BY-NC-ND license (http://creativecommons.org/licenses/by-nc-nd/4.0/).

1. Introduction

Due to advances in the remote-sensing technology of unmanned aerial vehicles (UAVs), UAVs have recently been applied in a wide range of fields, such as package delivery [1-3], military reconnaissance [4,5], post-disaster rescue [6], traffic monitoring [7], construction project quality inspection [8,9], and medical aid [10]. UAVs are typically small and highly mobile with a low cost, making them well suited for use in inspection and monitoring missions. Moreover, using UAVs to conduct such missions has the potential not only to greatly reduce labor investment but also to avoid some of the risks inherent to manual inspection processes. However, although there has been extensive research on the routing and scheduling optimization of UAVs performing inspection and monitoring tasks in various fields [11-14], little work has been

done on UAV-based inspection in engineering management, especially for mega-projects in engineering construction. This paper develops a novel approach to study the optimization of the inspection and monitoring mode of UAVs in an engineering project, with the aim of improving the quality and efficiency of engineering management.

In engineering construction, managers commonly need to perform multi-round inspection tasks within a certain construction area to dynamically screen out any hidden dangers—such as unlocked fences, cracks in concrete, or objects that could fall—that could result in major accidents. However, the application of the inspection approach adopted in the traditional artifactual field to engineering mega-projects can result in high labor costs, low inspection efficiency, and slow responses. In addition, it can be dangerous for people to carry out inspection tasks in areas featuring complex facilities or terrain. Fortunately, using UAVs for inspections effectively eliminates the above problems, as UAVs are a non-contact solution [15]. In addition, using UAVs in inspections

enables not only the collection of real-time images of monitoring sites within a short time but also the uploading of information to a cloud platform for historical archiving. Moreover, in order to meet periodic inspection demands, managers can use UAVs to visit monitoring sites repeatedly instead of having to manually perform inspections. Most importantly, UAV-based inspection prevents the managers of an inspection task from being put in danger.

Nevertheless, although UAV-based inspections are highly efficient in an engineering project, UAV battery limitations require managers to plan scientific inspection routes for UAVs by taking many factors into account. First, inspection missions cannot be completed by a single UAV powered by one battery, owing to the wide scope of inspections required in a construction project. Therefore, the scheduling of UAVs of multiple types and their charging demands must be considered. Second, a construction environment varies dynamically, so multi-round inspection tasks must be conducted to search for hidden dangers. Therefore, a scientific inspection route for UAVs must ensure not only that the UAVs return to charging stations before their power runs out but also that all monitoring sites are visited by the UAVs at intervals within a planning horizon (e.g., one day). Third, to prevent collisions between UAVs and engineering facilities, no-fly zones are needed to limit the route accessibility of UAVs traveling from one monitoring site to another. All the factors mentioned above impose significant constraints on the planning of inspection routing and scheduling for UAVs, greatly distinguishing such planning from the classical vehicle routing problem (VRP) encountered in traditional domains such as logistics and delivery services. In conventional VRP scenarios, UAVs must typically visit each customer point once within a known time window, with no instances of network inaccessibility between different customer points. However, in the context of our study, UAVs are required to make multiple visits to specific monitoring points within periodic time windows. Moreover, direct access between different monitoring points may be hindered due to the presence of construction structures and large equipment. In addition, decisions regarding UAV charging locations must be factored in. These complexities make the path planning for UAV inspection in engineering applications significantly more challenging than the standard UAV path-planning problems encountered in other domains. As a result, obtaining an optimal solution for small-scale problems becomes difficult, and even finding a feasible solution through experiential approaches becomes a formidable task for real-scale engineering projects. This distinction highlights the unique and demanding nature of UAV routing planning in the engineering domain, setting it apart from other UAV routing problems encountered in different fields.

Against this background, this paper explores the application of UAV-based inspection in engineering projects by considering the inspection routing and scheduling optimization of UAVs. A mathematical model and a tailored algorithm are designed for planning UAV inspection routes to search for hidden dangers in an engineering project. In contrast with classical vehicle routes for target surveillance or parcel delivery, where each customer or target is visited only once, UAV inspection routes for an engineering project require each UAV to visit monitoring sites in multiple rounds. Thus, consecutive inspection tasks for a given site need to be separated by a time window. In addition, a mathematical model is used to consider the limitations of electric batteries and no-fly zones in the planning of realistic and practical inspection routes that allow UAVs to monitor various sites. Due to the need for comprehensive consideration of the above factors and constraints, complex decisions must be made on monitoring task assignment and monitoring sequence scheduling for UAVs.

The scientific contribution of this paper is as follows. A mixed-integer linear programming (MILP) model is formulated to determine the inspection routing and scheduling of heterogeneous UAVs, with consideration of periodic inspection demands and charging and no-fly-zone constraints. A tailored algorithm based on a variable neighborhood search (VNS) is designed to solve the devised model, which can only be solved for small-scale instances by commercial solvers. In addition, numerical experiments are conducted to confirm the effectiveness of the model and the efficiency of the algorithm. Sensitivity analyses are performed to provide engineering managers with insights into inspection tasks. Furthermore, the Shiziyang Bridge (SZYB) project—a world-class engineering project—is used as an example of the application of the devised mathematical model and designed algorithm to inspection works in a real-life engineering project.

The remainder of this paper is organized as follows. The related work is reviewed in Section 2, while problem backgrounds for inspection routing and scheduling optimization in a mega-bridge project are elaborated in Section 3. The mathematical model and tailored algorithm are respectively described in Sections 4 and 5, and the experimental results are reported and discussed in Section 6. Section 7 presents the case study on the SZYB. Conclusions are then outlined in the last section.

2. Related works

In recent years, many studies have investigated the application of UAVs in various fields, from the perspectives of technology frameworks [16-19] and operational research [6,20,21]. This section reviews three streams of research: The first stream involves the application fields and tasks of UAVs; the second stream comprises the optimization of UAV routing and scheduling; and the third stream covers the optimization of inspection and monitoring tasks performed by UAVs.

The first research stream focuses on the application fields and tasks of UAVs. The tasks assigned to UAVs can be categorized as emergency management, product or package delivery, real-time monitoring and patrolling missions, and military combat missions. Chowdhury et al. [11] studied UAV inspection routing optimization for post-disaster management and developed a MILP model to minimize the post-disaster inspection cost for a disaster-affected area. Khan et al. [10] addressed the vital role of UAVs in the efficient delivery of first aid and medical supplies, and demonstrated the value of UAVs in a medical rescue response. Studies on package delivery have mainly focused on the scheduling of trucks and drones for cooperative delivery [2,22,23]. The last-mile delivery problem has been solved well by adopting a delivery mode of cooperative trucks and drones, according to the scheduling solution provided by scholars. Shen et al. [13] conducted a pioneering study on the application of UAVs in the monitoring of vessel air emissions, jointly optimizing routing and scheduling decisions for ship-deployed multiple UAVs in the monitoring of pollution from vessels. Rajan et al. [24] used a two-stage stochastic programming approach to optimize the routing problem of UAVs in the context of a patrolling mission, revealing the value of UAVs in information collection. In addition, Li et al. [7] investigated the UAV scheduling problem for the multi-period real-time monitoring of road traffic under demand uncertainty, where UAVs equipped with different imaging sensors are used for capturing multi-period target images of road traffic. An MILP model is formulated to minimize the operating cost of the UAVs. In the field of military combat missions, UAVs commonly perform target surveillance and reconnaissance missions, in which they depart from a depot and travel to targets to collect information, within their power limitations. Liu et al. [12] designed a hybrid optimization framework, in which the reconnaissance mission planning problem is decomposed into a target selection subproblem and a path-planning subproblem. The scholars devised an evolutionary algorithm and a

deep reinforcement learning method to respectively solve the target selection subproblem and the path planning subproblem. Although UAVs have been widely applied in medical, logistics, urban management, and military fields, there has been little discussion on applying UAVs to engineering fields, especially in terms of exploring the value of UAVs in engineering management. The present paper therefore explores the UAV routing and scheduling problem for an engineering project.

The second stream involves optimization research on UAV routing and scheduling problems. Most UAV routing and scheduling problems can be regarded as variants of the classical VRP or of the traveling salesman problem (TSP). However, decision-making in various scenarios with different targets varies greatly in the planning of the routing and scheduling of UAVs, in comparison with decision-making in the VRP and TSP. Xia et al. [20] studied routing planning for a fleet of UAVs collecting information from a set of regions in enemy territory within a given mission time window. The optimization objective was to maximize the total expected reward collected by the fleet. Similarly, Xu et al. [25] investigated multi-UAV cooperative routing planning within a complex confrontation environment. They developed a multi-constraint objective optimization model to ensure that each UAV reaches the mission area rapidly, reducing the possibility of a UAV being captured and destroyed. Other research [26,27] in the military field has considered joint planning of the routing and scheduling of UAVs and vehicles (i.e., the use of mobile charging vehicles or inspection-assisted vehicles). Zhen et al. [28] formulated an integer programming model to minimize the total time for completing monitoring tasks in a routing problem by adopting UAVs to monitor a set of areas with different accuracy requirements, thereby optimizing routing and scheduling for monitoring. Wang et al. [29] investigated the UAV monitor routing problem in the context of unattended offshore oil platforms. They established a multi-objective mathematical model with the shortest flight path and minimum correction times for intelligent UAVs. The field of logistic delivery involves the scheduling of multiple heterogeneous UAVs [21,30] and the joint planning of the routing and scheduling of UAVs and trucks [23,31]. The main optimization objectives are the sum of the waiting times of customers, the total distance traveled by the UAVs, the total delivery time of the UAVs, and the total cost of cooperative delivery. In the engineering management field, UAVs possess remarkable advantages for performing inspection and monitoring missions. Similar to the above-described applications of UAVs, the routing and scheduling of UAVs in an engineering project must be determined by considering the limitations of batteries and charging stations, the complexity of multiple heterogeneous UAVs, and the sets of monitoring areas. In addition, inspection routes must be planned for the collection of images of each monitoring site in multiple rounds at certain intervals, and terrain obstacles (i.e., construction facilities) that make routes inaccessible must be taken into consideration. However, no study has comprehensively considered the aforementioned factors along with a realistic decision demand, so there is a dearth of guidance for UAV inspection routing and scheduling decision-making in engineering projects.

The final stream reviews optimization works involving inspection and monitoring tasks. Huang et al. [32] investigated the bridge inspection routing problem. Unlike the traditional VRP, the bridge inspection problem must also consider the selection of overnight lodging accommodation for the inspection team, since the visited bridges are located over a large geographical area. Therefore, the inspection route not only needs to determine the sequence for visiting bridges but also the accommodation selection for lodging. Zhen et al. [33] studied an inspection routing problem with a background of coal mine safety personnel in underground mines, which was defined as a multi-depot VRP with time windows. Tasks and

workload balance, multiple inspector-vehicle docking sites, and the time windows for inspection tasks were considered in a MILP model. Similar to inspection tasks, routing optimization for patrolling missions [24] can be a novel VRP variant. The distinction lies in the fact that the patrolling missions must visit a set of targets in the initial routes and then a set of additional targets in the adjusted routes, when the information collected by UAVs is incomplete. As for monitoring tasks, the related optimization research [7,13,28] is commonly dedicated to minimizing the total monitoring time for completing the tasks. UAVs' data capacity for storing information, specific monitoring requirements for monitoring sites or areas, and the power limitation of UAVs are major factors that are considered in these studies' mathematical models. However, there is little optimization research on the routing problem associated with inspecting each monitored site at intervals with a fixed time window. Furthermore, unlike an environment in which no construction obstructs the flight paths of UAVs, an engineering construction site presents many obstacles. Thus, a no-fly zone is a novel constraint factor that needs to be considered when determining UAV inspection routing in an engineering project.

For a clearer picture, Table 1 [2,7,10−13,20−26,28,30,32] classifies the aforementioned studies in terms of the problem background, consideration, and solutions adopted. Compared with current operational research on the UAV routing and scheduling problem, this paper uses a novel insight to explore the UAV inspection routing problem in the field of engineering management and comprehensively considers charging decisions, the requirement for periodic monitoring, and no-fly zone constraints in a mathematical model. To the best of our knowledge, although the technologies for object identification and image collection are sufficiently mature for UAV inspection and monitoring tasks in engineering construction [15,34], there is a lack of research dedicated to UAV inspection routing and scheduling optimization in this particular field. Thus, this paper addresses this research gap by presenting a practical approach for solving the UAV inspection routing and scheduling problem in engineering projects.

3. Problem description

3.1. Problem background

We consider a set of monitoring sites to be inspected in multi-round monitoring by heterogeneous UAVs in a construction area. A fleet of UAVs with various performances (e.g., different flying velocities, battery capacities, and charging times) are required to visit each site at certain intervals to collect images to assist the engineering manager to screen for hidden dangers in a construction environment. The engineering manager must therefore assign inspection tasks to each UAV and plan corresponding routes through the monitoring sites. First, the inspection routes should ensure that each monitoring site is visited by a UAV at certain intervals (e.g., one day) within a planning horizon. Second, the inspection routes should ensure that the UAVs can return to a nearby charging station for charging before powering off. Finally, the inspection routes should prevent the UAVs from colliding with the construction facilities. Thus, there are no-fly zones that render some routes inaccessible. In addition, to simplify the problem, this paper considers two-dimensional (2D) UAV routes, so the flying altitude of the UAVs is approximately constant.

Fig. 1 depicts a procedure of UAV inspection routes in which two UAVs monitor four sites in a construction area. Two sites must be inspected in at least three rounds, and two other sites must be inspected in at least two rounds. The UAVs upload the images collected at each monitoring site to a cloud platform in real time. The managers responsible for the inspection missions then record the

L. Zhen, Z. Yang, G. Laporte et al.

Table 1
Overview of studies on the routing and scheduling of UAVs.

Application field	Factors considered					Objective	Solution methods	Ref.
	BL	HVL	CRP	MIR	U			
LD			✔			Delivery time	E&HA	[21]
		✔	✔			Delivery cost	EA	[23]
			✔			Delivery completion time	H	[2]
			✔			Delivery cost	H	[22]
	✔	✔				Multiple objectives with makespan, distance, etc.	H	[30]
MRM					✔	Travel cost of UAVs	H	[24]
	✔				✔	Collected information	H	[12]
	✔		✔			Investment cost and time window deviation.	H	[26]
		✔	✔			Travel cost of UAVs	H	[25]
		✔			✔	Collected information	EA	[20]
ER		✔	✔			Inspection cost of UAVs	H	[11]
		✔				Travel cost of UAVs	H	[10]
URI	✔					Inspection completion time	H	[28]
	✔			✔	✔	Travel cost of UAVs	E&HA	[7]
BI			✔			Inspection cost of UAVs	H	[32]
VEM						Inspection completion time	H	[13]
EPI	✔	✔		✔		Makespan of inspection mission	H	This paper

LD: logistic delivery; MRM: military reconnaissance missions; ER: emergency rescue; URI: urban road inspection; BI: bridges inspection; VEM: vessel emissions monitoring; EPI: engineering project inspection; BL: battery limitation; HVL: heterogeneous vehicle fleet; CRP: cooperative routing planning; MIR: multi-round inspection route; U: uncertainty; EA: exact algorithm; H: heuristic; E&HA: solution that combines exact and heuristic algorithm.
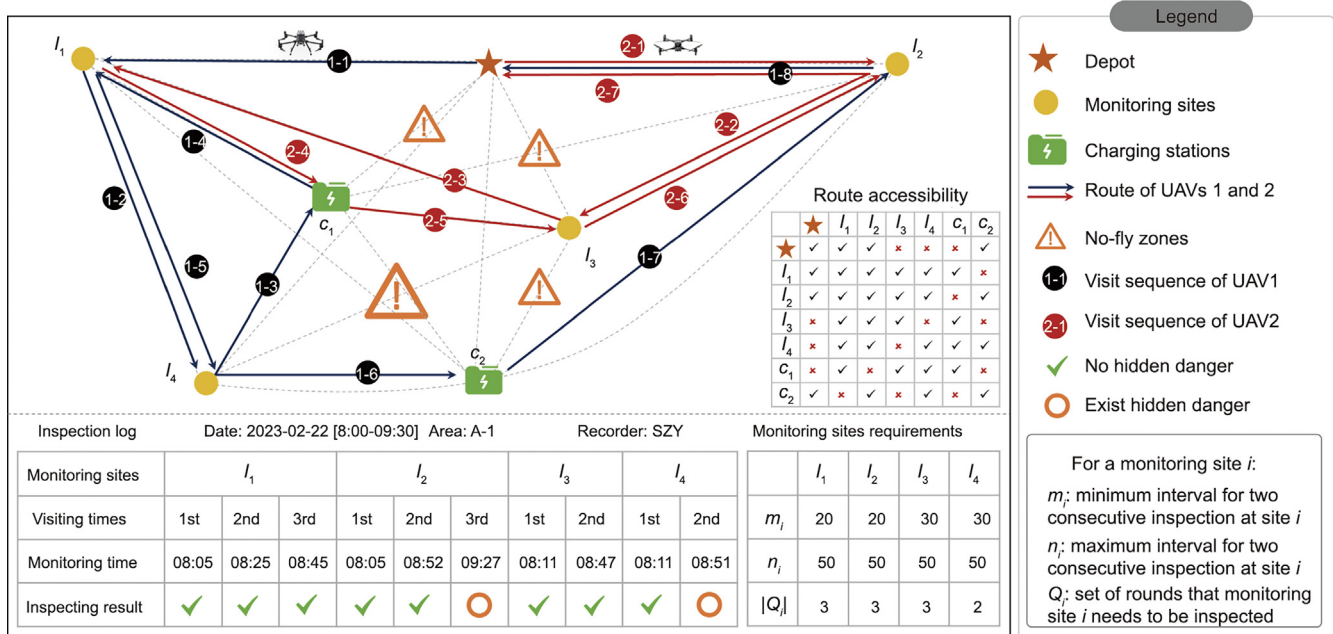

Fig. 1. An example of two UAVs performing inspection missions at four sites.

inspection results in logs (shown in the bottom part of the figure) to trace the construction safety of an area. If a hidden danger is detected at a monitoring site, the managers immediately issue a warning to the supervisors on site and guide them to inspect the situation and take measures to eliminate the hidden danger. Thus, UAV-based inspection not only reduces the labor cost of wide patrolling but also efficiently and dynamically discovers the hidden dangers of an engineering project through the optimization of the inspection routes.

Furthermore, Fig. 1 visually presents an illustrative example of solving the multi-round UAV inspection path-planning problem with charging decisions and the presence of unreachable paths. Taking UAV 1 as an example, after visiting monitoring points I1 and I4, the UAV first heads to charging station C1 to replenish its battery. Subsequently, UAV 1 performs the second round of inspections at points I1 and I4 before proceeding to charging station C2

for another battery recharge. Finally, after completing the third round of monitoring tasks at point I2, it returns to the starting point. In a conventional VRP problem, it might only be necessary to plan routes for the UAV to visit monitoring points I1, I4, and I2 once, separately. However, in the problem studied in this paper, the difficulty of planning UAV inspection routes significantly increases due to the following factors: ① The UAV route planning involves multiple visits to a single monitoring point, and the time windows for subsequent visits depend on the timing of previous visits. For example, if the first visit to I1 occurs at 8:05, the second visit should take place within the time window [8:25, 8:55] to monitor any changes in the point, and so on for subsequent visits. ② The existence of no-fly zones between different monitoring points requires rational assignment and access route planning for UAV inspection tasks. For example, after charging at C2, UAV 1 cannot access I3 but can only choose between I2 or I1. ③ Considering

the factors mentioned above, the UAVs can only recharge at reachable charging stations during their charging periods. Simultaneously, the flight time and charging time must not compromise the time window requirements of the next inspection task, making charging decisions equally complex and challenging. Fig. 1 only presents an example involving two UAVs visiting four monitoring points in three rounds, and the current complexity of the routes highlights the daunting nature of obtaining inspection paths for multiple heterogeneous UAVs visiting dozens of monitoring points in a large-scale problem.

Given the background of the above problem, the objective of an engineering manager is to determine the inspection routes of heterogeneous UAVs to minimize the total working time for completing multi-round inspection missions. By focusing on minimizing the total time, our research aims to address the critical need for efficient and effective UAV-based inspection routing and scheduling in engineering management. Achieving this objective aligns with the broader goal of optimizing construction project efficiency, reducing costs, and ensuring timely project completion. The challenges in this decision problem are that① battery limitations require a UAV to return to a charging station for recharging in the process of inspection, which complicates decision-making on inspection routes; ② no-fly zones constrain the accessibility of flying routes, complicating inspection task assignment and route planning; and ③ multi-round monitoring demand with a time window requires the scheduling of an inspection sequence and time for each monitoring site to satisfy rolling interval constraints, which complicates decision-making on routing and scheduling. An optimal solution should comprehensively address the abovementioned challenges and schedule an appropriate sequence for visiting each monitoring site in such a way that the time spent charging and waiting is as short as possible. In addition, no-fly zones sometimes result in detours that increase the inspection time, so the optimal solution should ensure that the UAVs fly from one site to the next (including the charging station) via the shortest route possible.

3.2. Assumptions

The following assumptions are made before formulating the mathematical model in Section 4:
(1) Each UAV performs monitoring missions at an approximately constant altitude. Thus, the vertical movement of the UAVs is not considered.
(2) All of the UAVs start flying from an origin site and fly to a destination site only after completing all their monitoring missions.
(3) The requirements for each monitoring site—such as the inspection-interval time window, the required monitoring time, and the number of inspection rounds—are known in advance.
(4) The flying distance of any pair of locations and the performances of the heterogeneous UAVs are known, as they are deterministic parameters.

4. Mathematical model

In this section, an MILP model is formulated for the integrated optimization problem. The objective is to minimize the total time—comprising the flying time, waiting time, inspection time, and charging time—for completing periodic inspection missions. As is usual practice for a transportation network formulation, the MILP model considers a direct connection for each origin−destination pair. The UAVs can fly from one node (where the nodes are the monitoring sites and charging stations) to another, provided that

there is no no-fly zone between the two nodes. The transportation time within a node is set to zero.

4.1. Notations

The set, parameters and decision variables used in the model are first outlined, show in the Table 2, and then the mathematical model is elaborated. For clarity, we use Roman and Greek letters to denote the parameters and decision variables, respectively.

4.2. Model formulation

The parameters and decision variables used in the model are outlined in the list of nomenclature, and then the mathematical model is elaborated. For clarity, we use Roman and Greek letters to denote the parameters and decision variables, respectively. Based on the input parameter and decision variables introduced above, we formulate the following mixed-integer programming model of this research.

$$[M0]\text{Minimize} \sum_{k \in K} \pi_k \tag{1}$$

subject to:

$$\sum_{k \in K} \alpha_{k,i,l} = 1 \qquad \forall i \in I, l \in Q_i \tag{2}$$

Table 2
Definitions of the sets, parameters, and decision variables of the mathematical model.

Items	Definition
Sets and subscripts	
K	Set of all UAVs, indexed by k, $k \in \{1, \cdots, |K|\}$.
I	Set of all monitoring sites, indexed by i, $i \in \{1, \cdots, |I|\}$.
B	Set of all charging stations, indexed by b, $b \in \{1, \cdots, |B|\}$.
$e, \dot{e}$	Origination and destination for all UAVs.
Q_i	Set of rounds that monitoring site i needs to be inspected $(i \in I \bigcup \{e, \dot{e}\})$, indexed by l, $l \in \{1, \cdots, |Q_i|\}, |Q_i| \leq Q$, Q is the maximum number of monitoring rounds for all UAVs.
Parameters	
T	Duration of the planning period.
r_k	Maximum battery capacity of UAV k.
h_k	Power consumption per unit distance of UAV k.
v_k	Average velocity of UAV k.
c_k	Charge power per unit time of UAV k.
$f_{i,j}^1$	Set to one 1 if there are no-fly zones between monitoring site i and monitoring site j, otherwise zero 0 $(i,j \in I \bigcup \{e, \dot{e}\})$.
$f_{i,b}^2$	Set to one 1 if there are no-fly zones between monitoring site i and charging station b, otherwise zero 0 $(i \in I \bigcup \{e, \dot{e}\}, b \in B)$.
$d_{i,j}^1$	Distance from monitoring site i to monitoring site j, $(i,j \in I \bigcup \{e, \dot{e}\})$.
$d_{i,b}^2$	Distance from monitoring site i to charging station b, $(i \in I \bigcup \{e, \dot{e}\}, b \in B)$.
$t_{k,i}$	Required time for completing the inspection task of site i for UAV k.
$g_{k,i}$	Required electricity to complete the inspection task of site i for UAV k.
m_i	Minimum interval for two consecutive inspections at site i.
n_i	Maximum interval for two consecutive inspections at site i.
M	A sufficiently large positive number.
Decision variables	
$\alpha_{k,i,l}$	Binary, equal to 1 if the lth inspection task of monitoring site i is completed by UAV k, otherwise 0.
$\beta_{k,i,l,j,l'}$	Binary, equal to 1 if UAV k completes the lth inspection task of site j immediately after finishing the lth inspection task of monitoring site i, otherwise 0.
$\varphi_{k,i,l,b}$	Binary, equal to 1 if UAV k flies to charging station b immediately after completing the lth inspection task of monitoring site i, otherwise 0.
$\lambda_{k,i,l}$	Time when UAV k starts the lth inspection task of monitoring site i.
$\theta_{k,i,l}$	Remaining electricity when UAV k starts the lth inspection task of monitoring site i.
π_k	Total operating time of UAV k, including the flying time, waiting time, inspection time, and charging time.

L. Zhen, Z. Yang, G. Laporte et al.   Engineering xxx (xxxx) xxx

$$\sum_{j \in I \bigcup \{\dot{e}\}} \sum_{l' \in Q_j} \beta_{k,i,l,j,l'} = \alpha_{k,i,l} = \sum_{j \in I \bigcup \{e\}} \sum_{l' \in Q_j} \beta_{k,j,l',i,l} \tag{3}$$
$$\forall k \in K, i \in I, l \in Q_i$$

$$\sum_{b \in B} \varphi_{k,i,l,b} \leq \sum_{j \in I \bigcup \{\dot{e}\}} \sum_{l' \in Q_j} \beta_{k,i,l,j,l'} \ \forall k \in K, i \in I, l \in Q_i \tag{4}$$

$$\sum_{j \in I \bigcup \{\dot{e}\}} \sum_{l' \in Q_j} \beta_{k,e,l,j,l'} = 1 \ \forall k \in K, l \in Q_e \tag{5}$$

$$\sum_{i \in I \bigcup \{e\}} \sum_{l \in Q_i} \beta_{k,i,l,\dot{e},l'} = 1 \ \forall k \in K, l' \in Q_{\dot{e}} \tag{6}$$

$$\beta_{k,i,l,j,l'} \leq f_{i,j}^1 + M \sum_{b \in B} \varphi_{k,i,l,b} \ \forall k \in K, i \in I \bigcup \{e\}, j \in I \bigcup \{\dot{e}\}, l \in Q_i, l' \in Q_j \tag{7}$$

$$\beta_{k,i,l,j,l'} \leq f_{i,b}^2 + M(1 - \varphi_{k,i,l,b}) \ \forall k \in K, i \in I \bigcup \{e\}, j \in I \bigcup \{\dot{e}\}, l \in Q_i, l' \in Q_j \tag{8}$$

$$\beta_{k,i,l,j,l'} \leq f_{j,b}^2 + M\left(1 - \varphi_{k,i,l,b}\right) \ \forall k \in K, i \in I \bigcup \{e\}, j \in I \bigcup \{\dot{e}\}, l \in Q_i, l' \in Q_j \tag{9}$$

$$\lambda_{k,i,l} + t_{k,i} + \frac{d_{i,j}^1}{v_k} \leq \lambda_{k,j,l'} + M(1 - \beta_{k,i,l,j,l'}) \ \forall k \in K, i \in I \bigcup \{e\}, j \in I \bigcup \{\dot{e}\}, l \in Q_i, l' \in Q_j \tag{10}$$

$$\lambda_{k,i,l} + t_{k,i} + \frac{d_{i,b}^2}{v_k} + \frac{(r_k - \theta_{k,i,l} + h_k d_{i,b}^2)}{c_k} + \frac{d_{b,j}^2}{v_k}$$
$$\leq \lambda_{k,j,l'} + M(2 - \varphi_{k,i,l,b} - \beta_{k,i,l,j,l'})$$
$$\forall k \in K, i \in I \bigcup \{e\}, b \in B, j \in I \bigcup \{\dot{e}\}, l \in Q_i, l' \in Q_j \tag{11}$$

$$\lambda_{k',i,l+1} \geq \lambda_{k,i,l} + t_{k,i} + m_i - M(2 - \alpha_{k,i,l} - \alpha_{k',i,l+1}) \ \forall k, k' \in K, i \in I, l \in Q_i / \{|Q_i|\} \tag{12}$$

$$\lambda_{k',i,l+1} \leq \lambda_{k,i,l} + t_{k,i} + n_i + M(2 - \alpha_{k,i,l} - \alpha_{k',i,l+1}) \ \forall k, k' \in K, i \in I, l \in Q_i / \{|Q_i|\} \tag{13}$$

$$\theta_{k,j,l'} \leq \theta_{k,i,l} - g_{k,i} - h_k d_{i,j}^1 + M(\sum_{b \in B} \varphi_{k,i,l,b} + 1 - \beta_{k,i,l,j,l'})$$
$$\forall k \in K, i \in I \bigcup \{e\}, j \in I \bigcup \{\dot{e}\}, l \in Q_i, l' \in Q_j \tag{14}$$

$$\theta_{k,j,l'} \geq \theta_{k,i,l} - g_{k,i} - h_k d_{i,j}^1 - M(\sum_{b \in B} \varphi_{k,i,l,b} + 1 - \beta_{k,i,l,j,l'})$$
$$\forall k \in K, i \in I \bigcup \{e\}, j \in I \bigcup \{\dot{e}\}, l \in Q_i, l' \in Q_j \tag{15}$$

$$\theta_{k,j,l'} \geq r_k - h_k d_{j,b}^2 - M\left(2 - \varphi_{k,i,l,b} - \beta_{k,i,l,j,l'}\right) \ \forall k \in K, i \in I \bigcup \{e\}, b \in B, j \in I \bigcup \{\dot{e}\}, l \in Q_i, l' \in Q_j \tag{16}$$

$$\theta_{k,j,l'} \leq r_k - h_k d_{j,b}^2 + M\left(2 - \varphi_{k,i,l,b} - \beta_{k,i,l,j,l'}\right) \ \forall k \in K, i \in I \bigcup \{e\}, b \in B, j \in I \bigcup \{\dot{e}\}, l \in Q_i, l' \in Q_j \tag{17}$$

$$\theta_{k,i,l} \geq g_{k,i} + h_k \min\{\min_{b \in B} d_{i,b}^2, d_{i,\dot{e}}^1\} - M(1 - \alpha_{k,i,l}) \ \forall k \in K, i \in I, l \in Q_i \tag{18}$$

$$\pi_k = \lambda_{k,\dot{e},0} - \lambda_{k,e,0} \ \forall k \in K \tag{19}$$

$$\alpha_{k,i,l} \in \{0, 1\} \ \forall k \in K, i \in I \bigcup \{e, \dot{e}\}, l \in Q_i \tag{20}$$

$$\beta_{k,i,l,j,l'} \in \{0, 1\} \ \forall k \in K, i \in I \bigcup \{e\}, j \in I \bigcup \{\dot{e}\}, l \in Q_i, l' \in Q_j \tag{21}$$

$$\varphi_{k,i,l,b} \in \{0, 1\} \ \forall k \in K, i \in I \cup \{e\}, b \in B, l \in Q_i \tag{22}$$

$$0 \leq \lambda_{k,i,l} \leq T \ \forall k \in K, i \in I \bigcup \{e, \dot{e}\}, l \in Q_i \tag{23}$$

$$0 \leq \theta_{k,i,l} \leq r_k \ \forall k \in K, i \in I \bigcup B \bigcup \{e, \dot{e}\}, l \in Q_i \tag{24}$$

$$0 \leq \pi_k \leq T \ \forall k \in K \tag{25}$$

Objective (1) minimizes the total time for all of the UAVs to complete the periodic inspection tasks, which comprises the flying time, waiting time, inspection time, and charging time. Constraints (2) ensure that each inspection task at each monitoring site is assigned to one and only one UAV. Constraints (3) are the flow-conservation constraints. Constraints (4) mean that, if a UAV needs to fly to a charging station for recharging, this operation is scheduled after the completion of an inspection task. Constraints (5) and (6) ensure that each UAV departs from the origin site and arrives at the destination site. Constraints (7) ensure that UAV k does not fly directly from monitoring site i to monitoring site j if there is a no-fly zone on the route from i to j. Constraints (8) and (9) mean that UAV k does not fly from monitoring site i to charging station b and then fly to monitor site j if there is a no-fly zone on the route from i to b or the route from b to j. Constraints (10) and (11) are fly-time conservation constraints for the UAVs. Constraints (12) and (13) ensure that the interval between two consecutive inspection tasks at one monitoring site is no shorter than the minimum interval time and no longer that the maximum interval time. Constraints (14) and (15) enforce power conservation when a UAV flies directly from one monitoring site to another monitoring site. Constraints (16) and (17) state that power is conserved when a UAV flies from a charging station to a monitoring site. Constraints (18) ensure that each UAV has sufficient power to travel to the destination site or the charging station closest to its current monitoring site. Constraints (19) compute the total time taken by a UAV to complete all of its inspection tasks. Constraints (20)–(25) define the decision variables.

5. Solution methodology

As is well known, the classical VRP is an NP-hard problem. The present study comprehensively considers the charging decisions, no-fly zone constraints, and periodic-interval time windows in a VRP framework. The initial model, M0, is therefore difficult to solve directly using CPLEX or other commercial solvers within an acceptable time, even for small-scale instances. Accordingly, this section develops a VNS-based metaheuristic for solving the model efficiently, based on the formulation and embedding of some simplified models. The advantages of the VNS mechanism lie in its ability to effectively explore diverse solution regions, avoid premature convergence to local optima, and improve the quality of solutions through iterative refinement. This makes the VNS particularly suitable for addressing NP-hard optimization problems such as the one proposed here.

5.1. Algorithm framework

Our problem can be divided into three subproblems: The first concerns the assignment of monitoring tasks (e.g., $\alpha_{k,i,l}$); the second concerns the scheduling of each UAV to carry out its task (e.g., $\beta_{k,i,l,j,l'}$); and the third concerns the determination of which

L. Zhen, Z. Yang, G. Laporte et al.

charging station each UAV should use for recharging after completing a monitoring task (e.g., $\varphi_{k,i,l,b}$). Since these three subproblems are intertwined, a non-optimized task-assignment plan could result in the monitoring interval constraints (12) and (13) not being satisfied, and a greedy scheduling plan could lead to the powering off of a UAV before it reaches a charging station or its next monitoring site. Therefore, a feasible initial solution must be generated to enable the model to be solved. In addition, effective neighborhood search strategies are needed to obtain improved solutions via iteration of the VNS algorithm. Finally, the charging decisions should be made from a global perspective, so that the performance of an inspection plan can be correctly evaluated.

To address the above-described challenges and solve the devised model, the VNS-based approach was implemented via the following steps.

Step 1: Initialize a feasible solution for conducting a neighborhood search.

Step 1.1: Obtain a feasible solution by iteratively solving the model M1_n.

Step 1.2: Set the best inspection plan (IP*) and the best objective value denoted as $F(\text{IP}^*)$, and set the local best inspection plan (IP̀) and local best objective value $F(\text{IP̀})$.

Step 2: Repeat the following steps until one of the termination conditions is satisfied.

Step 2.1: Explore the neighborhood to find a new solution (ĨP) based on IP̀ by adopting variable neighborhood descent (VND).

Step 2.2: Evaluate the new solution ĨP by solving the model M2 and obtain a new objective value, $F(\tilde{\text{IP}})$.

Step 2.3: If $F\left(\tilde{\text{IP}}\right) - F(\text{IP}^*) < 0$, set $\text{IP}^* = \text{IP̀} = \tilde{\text{IP}}$ and $F(\text{IP}^*) = F\left(\tilde{\text{IP}}\right)$.

Step 2.4: Generate a new feasible solution (IP̀) adopting the shaking procedure, and set $\tilde{\text{IP}} = \text{IP̀}$.

Step 3: Output the best inspection plan, IP*, and its best objective, $F(\text{IP}^*)$.

The stopping conditions are that ① the iteration count exceeds a threshold and ② $F(\text{IP}^*)$ has not been improved by a given threshold.

5.2. Initial solution generation

In this paper, the UAV inspection plan comprehensively considers the constraints of the time interval, power limitations, and no-fly zones. It is difficult to generate a feasible solution using heuristic rules without global considerations, because the local heuristic strategy struggles to balance the conflict between charging constraints and monitoring time interval constraints. In addition, compared with the classical electric vehicle routing problem (EVRP) and electric vehicle routing problem with time windows (EVRPTW), it is difficult to use the original model M0 to obtain a feasible solution within a short time using the CPLEX solver, given the expansion of the scale of the problem (as demonstrated in Section 6.2). We solve the problem in a rolling optimization manner to generate a feasible solution within a short time. Our core approach is to schedule the inspection routes for monitoring tasks one by one, according to the monitoring rounds (as shown in Fig. 2). The procedure of this approach is illustrated in Fig. 2. We denote the jth inspection task for monitoring site i as $i - j$, to clarify the task assignment in the following figures.

Each iteration solves a sub-model, M1_n ($n = 1, \ldots, \max_{i \in I}\{|Q_i|\}$), listed in Section S1 and Fig. S1 in Appendix A. The form of M1_n

is similar to that of the original model, M0. However, there is only one round of monitoring tasks that need to be conducted by a certain number of UAVs. The first iteration (solving model M1_1) can be regarded as solving a classical EVRP and the subsequent iteration as solving a classical EVRPTW (solving model M1_2 to M1_n) with a determined task assignment and routing sequence. A commercial solver cannot obtain the optimal solution within a short time but can generate a feasible solution within a reasonable time for conducting a neighborhood search.

5.3. Neighborhood structure

In the VNS process, diverse neighborhood structures must be considered in order to adequately explore the search space. We thus designed four strategies to find a new solution, while considering the problem characteristics of multiple monitoring rounds and no-fly constraints. We also consider the constraints of no-fly zones that limit route accessibility. Therefore, we first examine the route accessibility of a new solution. If the inspection route violates constraints (7)–(9), we search the corresponding neighborhood structure repeatedly until we obtain another new solution that does not violate constraints (7)–(9). A global tabu list is used to store the unsuccessful neighborhood searches and newly generated solutions, to avoid the need for repeated searches.

5.3.1. Strategy 1: Swapping monitoring tasks

Strategy 1 involves changing the inspection plan by swapping two monitoring tasks. Such a strategy can change a task assignment or monitoring sequence to obtain an improved inspection plan. Fig. 3 shows two options for applying Strategy 1 to search for a new solution. Under the first option, Strategy 1 changes the solution structure of $\alpha_{k,i,l}$ and $\beta_{k,i,l,j,l'}$. However, under the second option, Strategy 1 only changes $\beta_{k,i,l,j,l'}$. More specifically, taking option 1 as an example, $\alpha_{2,5,1}$, $\alpha_{1,3,2}$, $\beta_{2,5,1,4,2}$, and $\beta_{1,1,2,3,2}$ have a value of 1 in the initial solution and a value of 0 after the neighborhood search adopting Strategy 1. Subsequently, $\alpha_{1,5,1}$, $\alpha_{2,3,2}$, $\beta_{2,3,2,4,2}$, and $\beta_{1,1,2,5,1}$ are equal to 1.

5.3.2. Strategy 2: Inserting monitoring tasks

In contrast to Strategy 1, which keeps a constant total number of tasks assigned to a UAV, Strategy 2 changes the number of tasks assigned to a UAV because a better-performing UAV is sometimes able to complete more monitoring tasks than a poorer-performing UAV within the same period. In addition, Strategy 2 locally changes the sequence of a UAV to make the inspection route more scientific than it was before. The above two options are illustrated on the right and left of Fig. 4, respectively. When performing Strategy 2, we randomly select a monitoring task and insert it in a random location of the original sequence. The specific changes in the decision variables $\alpha_{k,i,l}$ and $\beta_{k,i,l,j,l'}$ during a neighborhood search are similar to those described in Section 5.3.1.

5.3.3. Strategy 3: Inserting monitoring rounds

Strategy 3 involves changing the solution by inserting monitoring tasks that belong to one monitoring round, thereby changing the task assignment and monitoring sequence from the perspective of the monitoring round. We use a monitoring-interval time window $[n_i, m_i]$ between two consecutive visits to a monitoring site. An optimal inspection plan should ensure that each UAV performs inspection work continuously—that is, a UAV waits as little as possible before performing its next round of monitoring at a site. Therefore, Strategy 3 randomly selects a round of monitoring tasks and reassigns some of the tasks to another UAV. In the example presented in Fig. 5, in the initial solution, the monitoring tasks 3-2, 4-2, and 2-2 are assigned to UAV 1 and are conducted after task
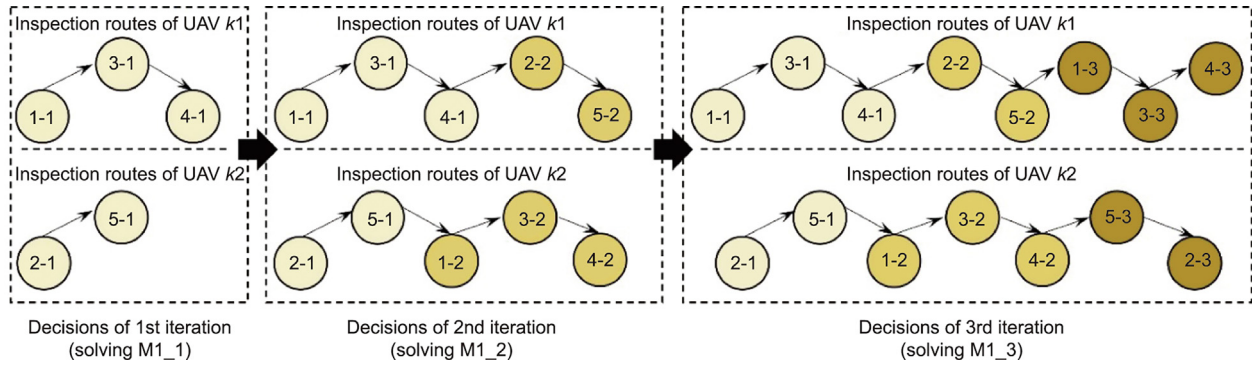
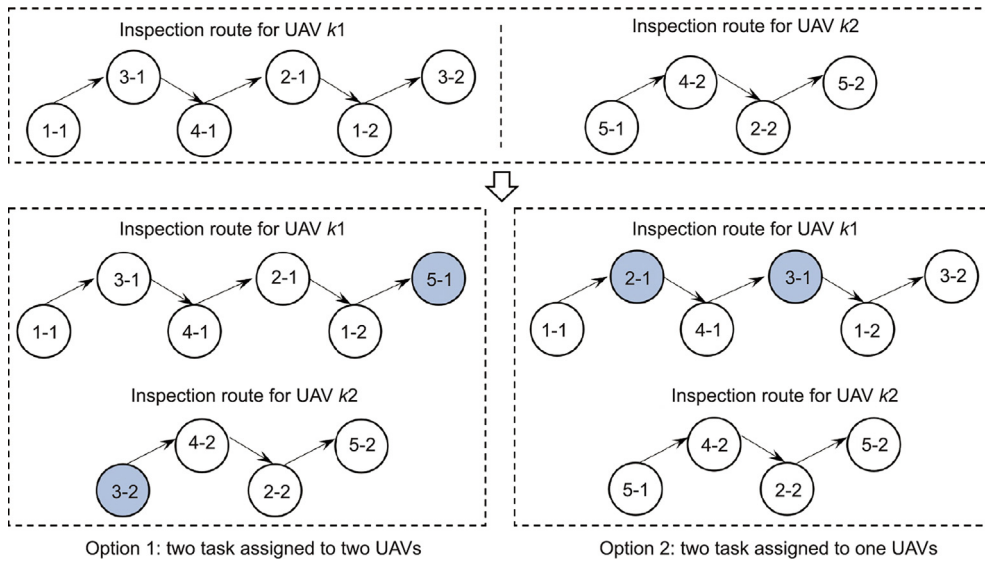**Fig. 2.** An example of the procedure for generating the initial inspection plan.

Fig. 3. Examples of neighborhood structure when swapping two monitoring task.
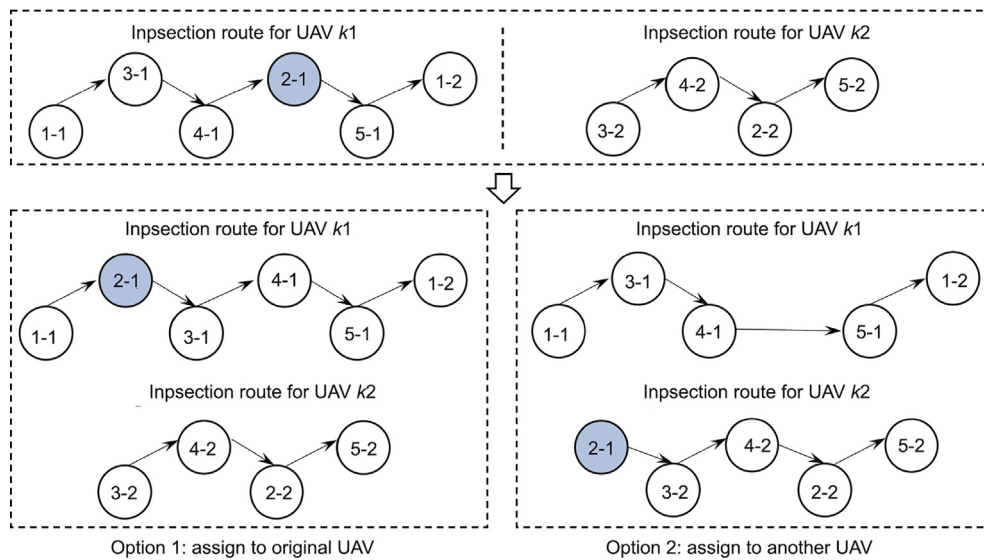

Fig. 4. Examples of neighborhood structure when inserting a monitoring task.

1-2. After the neighborhood search via Strategy 3, these tasks are inserted together into the start of the original sequence of UAV 2. The specific changes in the decision variables $\alpha_{k,i,l}$ and $\beta_{k,i,l,j,l'}$ during

the neighborhood search are similar to those described in Section 5.3.1. Strategy 3 finds an improved solution by assigning tasks to a better performing UAV and by optimizing the work continuity
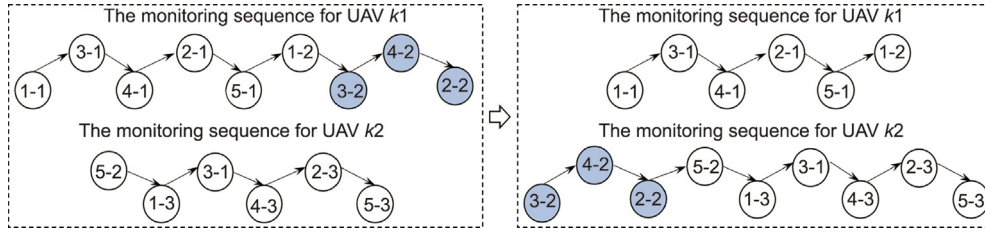
Fig. 5. Examples of neighborhood structure when inserting monitoring rounds.

through separating the inspection tasks belonging to different rounds.

5.3.4. Strategy 4: Swapping inspection routes

Strategy 4 involves changing the solution by swapping the inspection routes of two UAVs. Such a strategy is motivated by the consideration of heterogeneous UAVs. A better performing UAV can complete the same monitoring tasks within a shorter time than a poorly performing UAV. Fig. 6 shows an example of a neighborhood search adopting strategy 4. The use of strategy 4 affects the solution structure of $\alpha_{k,i,l}$. There are at most $|K|(|K|-1)/2$ neighborhood structures when $|K|$ UAVs perform the monitoring tasks. If all of the neighborhood structures have been searched for an input solution but no new solution has been generated, we use one of the other three strategies to search for a new solution.

5.4. VND framework

Using the neighborhood structures designed above, we devised a VND framework to search for an improved solution (the pseudo-code is given in Section S2 in Appendix A). The search procedure initially explores one neighborhood structure (i.e., it applies Strategy 1 to generate a new solution) and then extends to the next neighborhood structure if no better solution is found. Once a better solution is found in the current neighborhood structure, the procedure returns to the first neighborhood and reiterates the above searching procedure until one of the stopping conditions is met.

In the VND process, a simplified sub-model, M2, is used to evaluate the performance of the new inspection plan, as presented in Section S3 in Appendix A. The difference between models M2 and M0 is that the decision variables $\alpha_{k,i,l}$ and $\beta_{k,i,l,j,l'}$ are fixed in M2. In this way, most of the constraints—including the binary variables $\alpha_{k,i,l}$ and $\beta_{k,i,l,j,l'}$—are eliminated; the model retains only the binary variable $\varphi_{k,i,l,b}$ and the continuous variables $\lambda_{k,i,l}$, $\theta_{k,i,l}$, and π_k, and can be solved using a commercial solver within a short time, even for a large-scale instance. When the input inspection plan provides an infeasible solution, we set its objective value as M and continue to search for a new solution in the next neighborhood.

5.5. The shaking strategy: Regenerating a feasible solution

At the beginning of each iteration, the shaking procedure must avoid becoming trapped in a local optimum. Thus, the shaking strategy for generating a new feasible solution is designed as the following heuristic, which is illustrated in Fig. 7. In the first step, as far as possible, we assign the first round of inspection of each monitoring site to UAVs in a random but uniform manner in order to fix $\alpha_{k,1}$ for each monitoring site. We then solve model M1_1, given in Section 1 in Appendix A with the fixed variables $\alpha_{k,1}$ to generate the inspection route for the first round of monitoring tasks. Finally, we generate the inspection routes for the subsequent rounds through the rolling optimization process described in Section 5.2.

We take a problem with $|K|$ UAVs and $|I|$ monitoring sites as an example to illustrate the procedure for "assigning tasks in a random but uniform manner." We assign Q tasks of the first-round inspection (e.g., inspection tasks 1-1, 2-1, and 3-1) to UAVs one by one, in decreasing order of UAV velocity, until all of the monitoring tasks are assigned. Here, Q equals $\lceil |I|/|K| \rceil$. Thus, the task assignment variables $\alpha_{k,1}$ are fixed by adopting the above heuristic. However, the assignment plan for the following round of inspection tasks may be infeasible when iteratively solving the model M1_n ($n > 2$). Thus, we randomly change the number of tasks assigned to a UAV in the range of $[Q - \tau, Q + \tau]$, where τ is an integer parameter that is randomly generated in the range of $[1, \lceil Q/2 \rceil]$. We then repeat the above procedure until a new feasible solution is generated via the shaking strategy.

6. Numerical experiments

This section reports on the extensive numerical experiments conducted to assess the performance of the VNS algorithm; sensitivity experiments are also conducted to provide managerial insights. All the experiments were conducted on a workstation equipped with two Intel Xeon Gold 5218R CPUs running at 2.10 GHz with 32 GB of memory on a Windows 10 operating system. The algorithm and models were programmed in C# (Visual studio 2022), and CPLEX 12.6.1 was used as the MILP solver. Considering
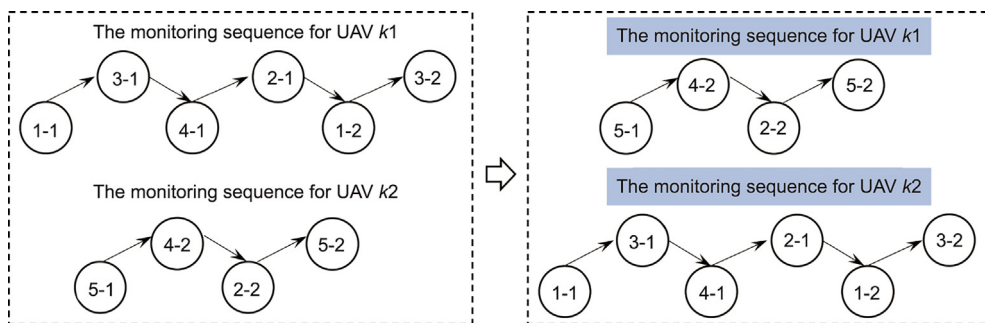

Fig. 6. Examples of neighborhood structure when swapping monitoring sequence.
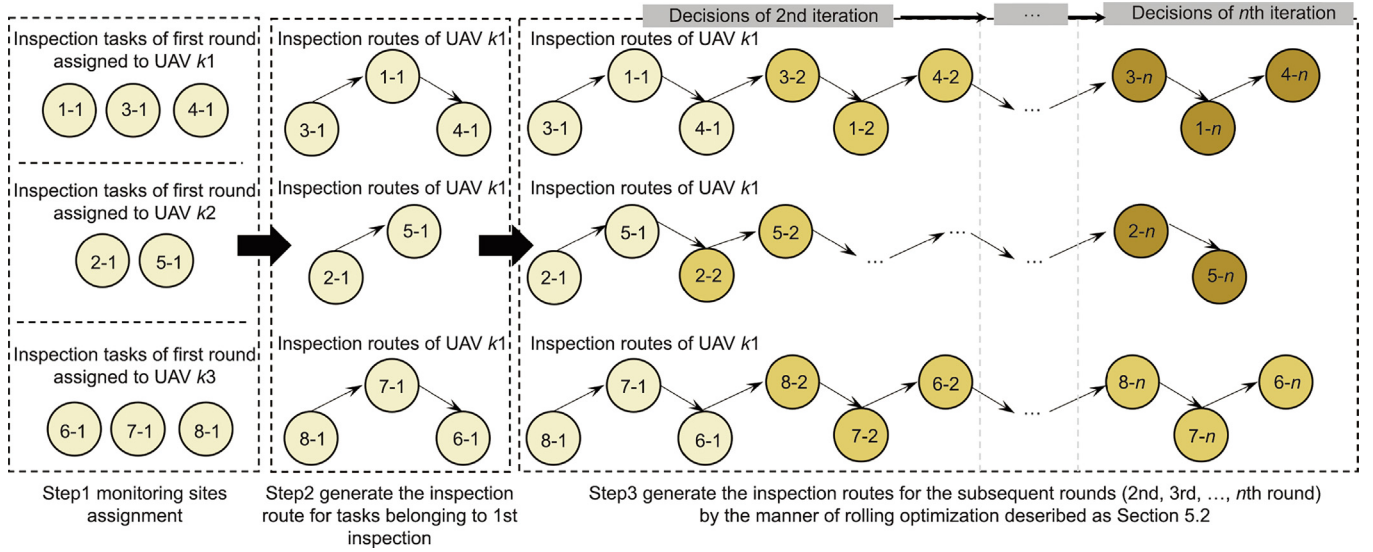
Fig. 7. Example of the shaking strategy.

that daily monitoring sites dynamically vary during construction (i.e., the sites can change daily), the design of a UAV inspection routing and scheduling plan should not be time consuming. The time limit was thus set to 3600 s to satisfy the demands of practical decision planning.

6.1. Generation of test parameters

Instances were generated to simulate a series of scenarios in which UAVs carry out inspection tasks in an engineering project. In practice, inspection tasks are normally performed during periods of construction work (e.g., from 8 to 12 h or from 14 to 17 h), and monitoring sites can be different in the morning and afternoon (or night). In addition, different construction areas have different types of hidden dangers that need to be monitored via UAVs. Thus, the present study took 4 h as a planning horizon ($|T|$) for determining the inspection plan for UAVs. Monitoring sites and charging stations were distributed over a square area of 100 km^2, and the Euclidean distance was calculated as the distance between any two nodes for a UAV. Regarding the performance of the UAVs used for inspection, Table 3 gives the parameter settings of the UAVs, with reference to the M300 RTK UAV of Dajiang Company [35]. The interval time windows of different monitoring sites were set as $\left[0.5 \times \frac{|T|}{\max\limits_{i \in I}\{|Q_i|\}}, \frac{|T|}{\max\limits_{i \in I}\{|Q_i|\}}\right]$ to enable the UAVs to search for hidden construction dangers at monitoring sites periodically over one planning horizon. The number of no-fly zones affects the route accessibility for the UAVs, and it was assumed that 20% of all arcs were inaccessible because of no-fly zones.

Based on the settings given in Table 3, we generated nine instance groups (ISGs) to assess the efficiency of our algorithm. Table 4 gives the key parameter settings of the different ISGs. ISG1, ISG2, and ISG3 were regarded as small-scale instances;

ISG4, ISG5, and ISG6 were regarded as medium-scale instances; and ISG7, ISG8, and ISG9 were regarded as large-scale instances.

6.2. Investigation of the solution quality of the algorithm

The first series of numerical experiments were conducted on small-scale instances to compare the results obtained using the CPLEX solver, the VNS-based metaheuristic, and the initial generation strategy introduced in Section 5.2. Table 5 provides a comparison of the results for the objective value and the computing time, showing that CPLEX obtained an optimal solution only for the first two small-scale ISGs (i.e., ISG1 and ISG2) within 3600 s. In contrast, our algorithm obtained the same solution for ISG1 and ISG2 within 30 s. When CPLEX could not obtain the optimal solution within 3600 s, we compared its upper-bound solution value with the solution value of our algorithm. The average difference between the two values was −13.86%, and the computing time of the devised algorithm was less than 120 s, indicating that it obtained a better solution than the CPLEX solver within a short time for the ISG3 problem scale. In addition, the average differences between the solutions of the devised algorithm and the initial generation strategy for ISG1, ISG2, and ISG3 were 17.54%, 17.56%, and 23.85%, respectively. The neighborhood structures described in Section 5.3 were therefore effective in finding improved solutions within the VND search framework.

The second series of numerical experiments were conducted on the medium-scale instances. Table 6 shows that our algorithm obtained a solution far better than that obtained by CPLEX within 3600 s (with the average difference being −30.74%). With increases in the number of monitoring sites and monitoring rounds, CPLEX could not obtain a feasible solution for ISG5 and ISG6 within 3600 s, whereas the devised algorithm solved the model within 300 s. In addition, the average difference between the solutions of the devised algorithm and the initial generation strategy on

Table 3
Parameter setting for heterogeneous UAVs.

Parameter	Range setting	Unit	Parameter	Range setting	Unit
r_k	[5000,7000]	mA	c_k	[6000,6400]	mA·h^{-1}
h_k	[180,220]	mA·km^{-1}	$t_{k,i}$	[0.03,0.05]	h
v_k	[35,36]	km·h^{-1}	$g_{k,i}$	[200,400]	mA·h^{-1}

Table 4
Key parameter settings for different problem ISGs.

Group ID	No. of UAVs ($|K|$)	No. of monitoring sites ($|I|$)	No. of charging stations ($|B|$)	No. of maximum monitoring rounds ($|Q|$)	Duration of planning horizon ($|T|$)
ISG1	2	4	3	2	4
ISG2	2	5	3	2	4
ISG3	2	6	3	3	4
ISG4	3	7	3	3	4
ISG5	3	8	3	3	4
ISG6	4	9	3	4	4
ISG7	5	12	4	4	4
ISG8	5	14	4	4	4
ISG9	6	16	5	4	4

No.: number.

Table 5
Algorithm performance for small-scale instances.

Instance		CPLEX		Strategy (Obj (h))	VNS		Gap	
Group	ID	Obj (h)	Time (s)		Obj (h)	Time (s)	Gap1	Gap2
ISG1	1	1.39	8	1.66	1.39	24	0	20.03%
	2	1.51	7	1.83	1.51	13	0	21.28%
	3	1.45	8	1.75	1.45	13	0	20.57%
	4	1.78	13	1.94	1.78	15	0	9.29%
	5	1.71	9	2.05	1.71	12	0	19.87%
ISG2	1	1.59	143	1.82	1.59	12	0	14.80%
	2	1.66	91	1.94	1.66	10	0	17.25%
	3	1.53	294	1.90	1.53	25	0	24.37%
	4	1.61	186	1.79	1.61	13	0	11.51%
	5	1.56	271	1.87	1.56	19	0	19.86%
ISG3	1	3.66	> 3600	3.82	2.91	30	−20.56%	31.46%
	2	3.85	> 3600	3.88	3.23	86	−16.04%	19.93%
	3	3.79	> 3600	4.14	3.19	25	−15.72%	29.71%
	4	3.78	> 3600	3.72	3.09	46	−18.28%	20.38%
	5	3.91	> 3600	3.97	3.37	23	−13.64%	17.75%

Gap1 and Gap2 represent the optimality gap between the objective values of the solutions obtained by CPLEX, the initial generation strategy, and the VNS-based solution approach, respectively; > 3600 means that the computing time for obtaining the optimal solution for CPLEX is more than 3600 s; Obj represents the objective value of the proposed model solved by each solution methodology; ID represents the different instances for the same instance size.

Table 6
Algorithm performance for medium-scale instances.

Instance		CPLEX		Strategy (Obj (h))	VNS		Gap	
Group	ID	Obj (h)	Time (s)		Obj (h)	Time (s)	Gap1	Gap2
ISG4	1	5.53	> 3600	4.70	4.23	76	−23.61%	11.16%
	2	4.39	> 3600	3.99	3.18	72	−27.51%	25.45%
	3	6.11	> 3600	4.55	3.64	74	−40.33%	24.93%
	4	6.27	> 3600	4.76	4.32	89	−31.04%	10.10%
	5	4.55	> 3600	3.91	3.13	79	−31.18%	24.64%
ISG5	1	—	> 3600	7.06	6.16	134	—	14.56%
	2	—	> 3600	5.23	4.65	187	—	12.35%
	3	—	> 3600	5.39	4.80	177	—	12.23%
	4	—	> 3600	7.13	6.28	74	—	13.50%
	5	—	> 3600	6.35	4.99	174	—	27.22%
ISG6	1	—	> 3600	8.33	6.50	288	—	28.27%
	2	—	> 3600	5.18	4.40	197	—	17.75%
	3	—	> 3600	7.85	6.72	166	—	16.90%
	4	—	> 3600	8.56	6.86	155	—	24.87%
	5	—	> 3600	5.59	4.50	218	—	24.20%

Dash means that the computation time of CPLEX for obtaining a feasible solution exceeds 3600 s. Gap1 and Gap2 represent the optimality gap between the objective values of the solutions obtained by CPLEX, the initial generation strategy, and the VNS-based solution approach, respectively. > 3600 means that the computing time for obtaining the optimal solution for CPLEX is more than 3600 s. Obj represents the objective value of the proposed model solved by each solution methodology. ID represents the different instances for the same instance size.

the medium-scale instances was 19.21%, which confirms the good performance of the VNS-based metaheuristic in searching for better solutions.

The third series of numerical experiments were conducted on the large-scale instances. As the CPLEX solver could not obtain a feasible solution within a reasonable time on large-scale instances,

Table 7 gives the differences between the solutions (i.e., Gap2) obtained via the VNS-based approach and the initial generation strategy. The average value of Gap2 was 21.87%, which was greater than the values for the medium-scale instances (19.21%) and the small-scale instances (19.65%). This result indicates that our algorithm was stable and effective in finding the best solution for dif-

Table 7
Algorithm performance for large-scale instances.

Instance		Strategy (Obj (h))	VNS		Gap (Gap2)
Group	ID		Obj (h)	Time (s)	
ISG7	1	10.41	8.24	947	26.45%
	2	9.91	7.73	731	28.19%
	3	10.92	8.69	553	25.61%
	4	12.92	10.60	617	21.87%
	5	9.69	8.39	1029	15.46%
ISG8	1	12.94	10.72	1872	20.63%
	2	10.69	8.62	1495	24.05%
	3	11.16	9.40	878	18.74%
	4	10.47	8.36	1343	25.29%
	5	10.60	8.96	845	18.31%
ISG9	1	13.56	10.77	1684	25.91%
	2	14.32	11.64	1482	23.06%
	3	12.56	10.68	1194	9.44%
	4	13.25	11.95	1560	10.89%
	5	14.78	11.73	2548	25.97%

Gap2 represents the gap between the solutions obtained via optimality and the initial generation strategy. Obj represents the objective value of the proposed model solved by each solution methodology. ID represents the different instances for the same instance size.

ferent instances sizes. Most importantly, the computing times required for solving the nine ISGs were much shorter than 3600 s, indicating that our algorithm can effectively help an engineering manager plan a UAV inspection for application in a dynamically changing engineering schedule.

6.3. Derivation of managerial insights from sensitivity analyses

This subsection reports on sensitivity analyses performed to derive managerial insights into optimizing the planning of UAV inspections. The sensitivity analyses were conducted from two perspectives: The first was the number of UAVs, and the second was the speed of the UAVs.

6.3.1. Sensitivity analysis of the number of UAVs used for the inspections

The number of UAVs used for inspections affects the total working time of the UAVs. However, too many UAVs could result in low efficiency (e.g., only a few inspection tasks being assigned to a UAV), whereas too few UAVs could require a long time being needed to complete all of the inspection tasks (e.g., the UAVs need to recharge frequently during the process of inspection). It is thus necessary for an engineering manager to determine the suitable number of UAVs to use for conducting inspection tasks. We took the small-scale instances (ISG1, ISG2, and ISG3) as examples to investigate the relationship between the number of UAVs and the total working time. In addition, we excluded the effect of the UAV performance (e.g., the velocity or battery capacity) by assuming that the performance of the UAVs was homogeneous when changing the number of UAVs. Fig. 8 shows the effect of the num-

ber of UAVs used for the inspections on the total working time. It can be seen that the use of two UAVs was suitable for ISG1 and ISG2 and the use of five UAVs was suitable for ISG3.

The above results indicate that, on the scale of ISG1 and ISG2, two UAVs were sufficient to complete all of the inspection tasks. Thus, investing in more UAVs to conduct the same number of inspection tasks would increase the total working time with no gain, as this would simply increase the amount of unnecessary flying time and prolong the waiting time. However, the maximum number of monitoring rounds and number of monitoring sites are both much larger for ISG3 than for ISG1 and ISG2, and the UAVs thus need to perform more inspection tasks at the same number of monitoring sites for ISG3 than for ISG1 and ISG2. Thus, increasing the number of UAVs for inspection tasks for ISG3 would reduce the total working time for completing all of the inspection tasks. These results reveal to an engineering manager that it is necessary to consider an appropriate ratio of the number of UAVs for inspection to the total number of inspection tasks, and that this ratio is affected by the performance of the UAVs and the range of inspection areas.

6.3.2. Sensitivity analysis of the variation in UAV performance

The performance of the UAVs used for the inspections greatly affects their total working time. This subsection discusses the effect of variations in different parameters of UAVs on their total working time, thereby showing each parameter's importance in terms of reducing the total working time. The battery power (r_k), average velocity (v_k), and power consumption per unit distance (h_k) were the three parameters considered in the sensitivity experiment. To explore the importance of variations in these three
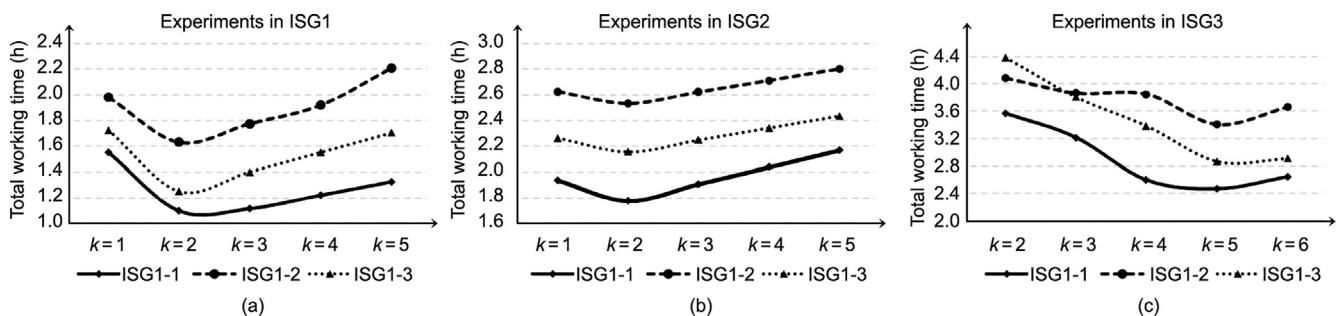

Fig. 8. Sensitivity analysis of the number of UAVs for the inspections.

parameters, we set a benchmark for each and varied the parameters from their benchmark settings by −20% to 20%. In addition, it is intuitive that, compared with a UAV traveling at a lower speed, a UAV traveling at a higher speed requires more power, which means that the power consumption per distance increases at a higher speed. We thus made the variation in h_k the same as that in v_k when changing the average velocity of a UAV. The above three parameters were varied on the scales of ISG1, ISG2, and ISG3; the results are shown in Fig. 9.

These experiments provided interesting insights. First, increasing only the battery power above a threshold decreased the total working time, due to a decrease in the charging time. Second, increasing the average velocity of the UAVs did not always reduce the total working time when there were a low number of monitoring tasks and a low maximum number of monitoring rounds (Figs. 9 (a) and (b)). This is because the power consumption per unit distance typically increases with the average velocity for the current technology standard, resulting in an increase in the time spent charging or waiting. However, increasing the velocity of the UAVs was an effective way to shorten the total working time when there were many inspection tasks (at least up to the scale of ISG3). Finally, an increase in power consumption per unit distance resulted in an increase in the working time required to complete the inspection tasks. This is because an increase in power consumption per unit distance results in a decrease in the distance that a UAV can fly within one charging cycle. The above analysis should be helpful to a project manager purchasing UAVs for inspection tasks in an engineering project, as it shows that, in order to effectively improve the efficiency of inspection works, UAV velocity should be the primary consideration, followed by UAV endurance.

6.4. Experimental summary

In this section, we report on a comprehensive set of numerical experiments that were conducted to evaluate the performance of the VNS algorithm in solving the UAV inspection routing and scheduling problem. The efficiency of the VNS algorithm was assessed through three series of experiments, involving small, medium, and large-scale instances. The results were compared with those obtained using the CPLEX solver and an initial generation strategy. The VNS algorithm consistently outperformed CPLEX in terms of solution quality and computing time. For small-scale instances, the VNS algorithm achieved similar solutions to CPLEX but with significantly faster computation times. For medium-scale instances, the VNS algorithm obtained substantially better solutions compared with CPLEX. For large-scale instances, where CPLEX was infeasible within a reasonable time, the VNS-based approach delivered stable and effective solutions.

Furthermore, sensitivity analyses were performed to gain insights into the optimization of UAV inspection planning from two perspectives: the number of UAVs and the UAVs' speed. For small-scale instances, two UAVs were found to be sufficient; for larger instances, a higher number of UAVs resulted in a reduced total working time. In addition, the average velocity of the UAVs was shown to be a crucial factor in shortening the total working time, especially for scenarios with numerous inspection tasks. On the other hand, an increase in power consumption per unit distance resulted in longer working times due to the reduced flight distance per charging cycle.

The results from the sensitivity analyses provide valuable guidance for engineering managers planning UAV inspections in dynamically changing engineering schedules. By considering an appropriate ratio of UAVs to inspection tasks and prioritizing UAV speed, managers can optimize the efficiency of inspection operations. These findings contribute to the effective application of UAVs in engineering projects, allowing for timely and comprehensive monitoring of construction areas while minimizing planning efforts.

7. Case study

In this section, the SZYB engineering project is taken as an example of the use of the devised model and algorithm to decide on an inspection plan. As the SZYB is still under construction, it provides a simulated real-world problem scale for our investigation. Numerical experiments were conducted using real-world parameter settings, and several analyses were performed.

7.1. Case background

As mentioned in Section 1, the UAV-based inspection approach has great advantages for performing inspection tasks in a complex and high-risk construction environment in order to continuously screen out potential hidden dangers (as illustrated in Fig. 10). The proposed mathematical model and algorithm provide a scientific tool for a project manager to determine an inspection plan for UAVs (inspection tasks assignment, monitoring sequence, and charging decisions). Thus, in order to demonstrate the practical application of our solution approach for determining an inspection plan for UAVs, we take SZYB as a case study and simulate the decision-making based on estimated data from real-world cases.

The SZYB crosses the Pearl River and has a length of 2180 m. It is located in Guangzhou, Guangdong Province, and serves as an engineering control project of the Shiziyang Channel dedicated to strengthening the connectivity of the surrounding cities and regions. Fig. 11 shows the approximate location and provides a concept illustration of the SZYB. Such an ultra-large span, high
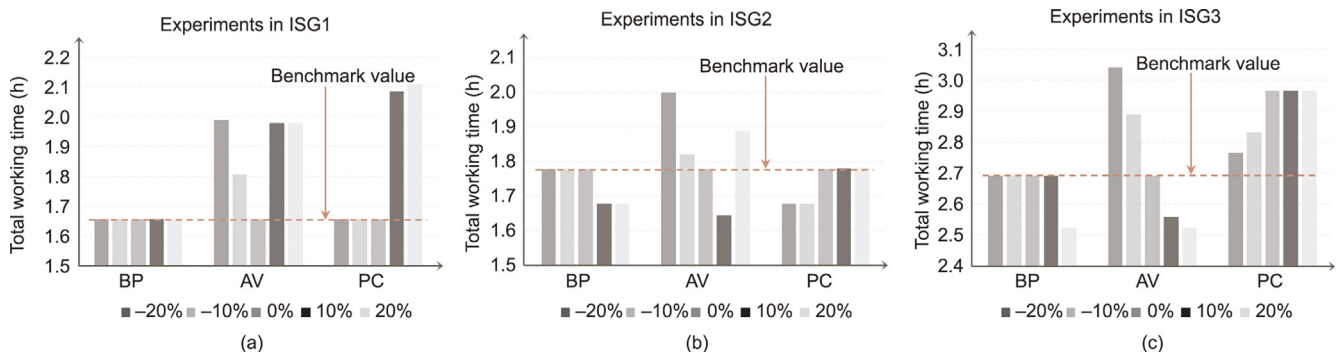

Fig. 9. Sensitivity analysis on the variation of UAVs' performance. BP denotes the variation of battery power; AV denotes the variation of average velocity; PC denotes the variation of power consumption per unit distance.
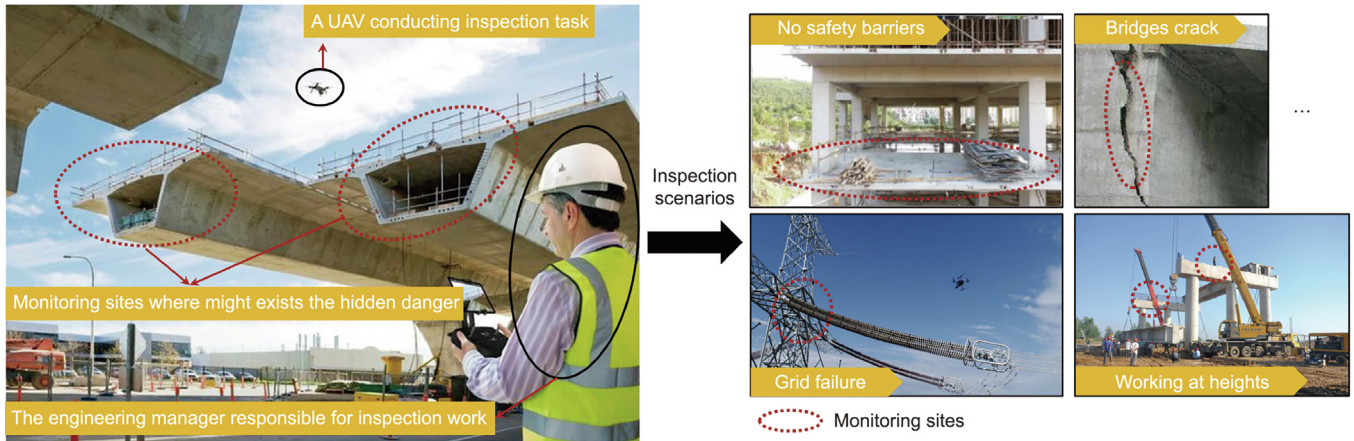
Fig. 10. Application of the UAV-based inspection approach in engineering management.

Fig. 11. A concept illustration of SHYB.

load, and ultra-wide deck suspension bridge is technically difficult to construct to a world-class standard. Moreover, there are additional difficulties associated with the construction of the SZYB, since its engineering characteristics such as the ultra-large scope of construction, high technical difficulties, and long construction period mean that there are many construction areas at high risk throughout the construction cycle. It is therefore essential for project managers to carry out continuous screening operations to identify hidden dangers and hence reduce the incidence of major accidents.

7.2. Case results

This subsection describes the parameter settings based on estimation data for the real-scale case of the SZYB. The performance of the devised approach for solving the real-world instance is as follows.

7.2.1. Performance in solving the real-scale instance

The parameter settings for the real-world instance were first clarified before we conducted numerical experiments to validate the efficiency of the devised algorithm in solving our model. According to planning files kept by the Department of Transport of Guangdong Province [36], the construction areas of the SZYB could be approximately simulated as a 12-km-long and 2-km-wide rectangle (as illustrated in Fig. S2 in Appendix A). We estimated a likely problem scale that was much larger than the scale

of ISG9 for determining the UAV inspection plan in the case of the SZYB, where a problem scale that associated to eight UAVs, 22 monitoring sites, four monitoring rounds and six charging stations. We refer to this new instance group as ISG10. The other parameters were set to be the same as those in Section 6.1. The following computing results were obtained for ISG10 and from the problem simulation shown in Fig. S2.

Table 8 shows that the devised algorithm obtained the best solution for most of the real-world instances within 3600 s. There was an average difference of 23.64% between the results obtained using the devised algorithm and those obtained using the strategy described in Section 5.2. These results confirmed the efficiency of the devised algorithm in solving a real-world instance. The calculated gap value highlights the significance of improving a multi-round inspection task assignment and visiting sequences from a global optimality perspective to enhance the efficiency of inspection tasks. Thus, when planning path routing for tasks requiring multiple visits to monitoring points, it is crucial to consider the UAVs' task assignments and visiting sequences holistically. Such considerations can have a substantial impact on the overall inspection time.

To expedite the computation time for solving the devised model to significantly below the 3600-s threshold, a potential strategy involves partitioning the monitoring sites into a series of smaller areas. Specifically. More specifically, the monitoring sites could be clustered into four rectangular regions, each measuring 4 km in length and 2 km in width. Subsequently, the devised model

L. Zhen, Z. Yang, G. Laporte et al.

Table 8
Results from solving the proposed model for the real-scale instance.

Instance		Strategy (Obj (h))	VNS		GAP (Gap2)
Group	ID		Obj (h)	Time (s)	
ISG10	1	15.87	12.69	2403	25.08%
	2	14.12	11.67	1900	20.95%
	3	14.29	11.70	3447	22.09%
	4	14.53	11.42	2271	27.15%
	5	15.66	12.74	2697	22.92%

Table 9
Timetable of inspection work for the real-world instance illustrated in Fig. S1.

UAV	Inspection tasks in the 1st round		Inspection tasks in the 2nd round		Inspection tasks in the 3rd round		Inspection tasks in the 4th round	
	I_index	I_time	I_index	I_time	I_index	I_time	I_index	I_time
1	0	8:53	2	9:27	2	10:05	2	10:38
	2	8:54	3	9:31	3	10:09	3	10:42
	3	8:58	9	9:37	16	10:16	9	10:49
	9	9:04	13	9:41	13	10:21	13	10:53
	13	9:09	—	—	—	—	—	—
	21	10:59	—	—	—	—	—	—
2	0	8:30	10	9:09	17	9:58	17	10:31
	17	8:36	17	9:20	14	10:04	14	10:36
	6	8:41	14	9:25	18	10:09	18	10:42
	14	8:47	18	9:31	8	10:26	12	10:46
	18	8:52	12	9:36	—	—	—	—
	12	8:56	—	—	—	—	—	—
	7	9:03	—	—	—	—	—	—
	8	9:06	—	—	—	—	—	—
	21	10:51	—	—	—	—	—	—
3	0	9:51	8	9:54	12	10:08	10	10:13
	21	10:19	—	—	—	—	—	
4	0	10:26	—	—	5	10:27	1	10:48
	21	11:04	—	—	7	10:30	6	10:54
	—	—	—	—	—	—	—	—
	—	—	—	—	—	—	—	—
5	0	8:57	1	9:23	11	10:06	11	10:46
	11	9:01	11	9:34	9	10:10	16	10:51
	16	9:09	6	9:38	1	10:16	5	11:00
	5	9:17	16	9:43	6	10:21	7	11:03
	21	11:11	5	9:52	—	—	—	—
	—	—	7	9:58	—	—	—	—
	—	—	15	9:09	—	—	—	—
6	0	8:00	20	9:16	15	9:09	15	9:45
	15	8:05	19	9:19	20	9:16	20	9:49
	20	8:09	4	9:28	19	9:19	19	9:52
	19	8:12	10	9:41	4	9:28	4	10:00
	1	8:21	—	—	10	9:41	—	—
	4	8:24	—	—	—	—	—	—
	10	8:31	—	—	—	—	—	—
	21	10:10	—	—	—	—	—	—

I_index and I_time denote the index of different monitoring sites and the corresponding monitoring time, respectively. The time for monitoring sites "0" and "21" indicate the departure time of the corresponding UAV from the origination and the arriving time at the destination, respectively. The planning horizon is set as 8 h to 12 h in the above experiment.

and algorithm could be employed to determine the inspection plan for each corresponding area individually. This would entail solving four subproblems simultaneously, each involving two UAVs, five or six monitoring sites, and two charging stations. While this approach may incur some loss of optimality due to the separate solving of medium-scale problems, it would serve as a practical solution for reducing the computation time in real-world instances with numerous monitoring sites. Notably, the computing time for each medium-scale instance has been validated to be no more than 5 min, as corroborated in the experimentation results (shown in Table 6). However, the development of an effective method for clustering monitoring sites into different sub-areas is left as a subject for future research aimed at mitigating the extent of optimality loss.

7.2.2. Practical application of our approach for making an inspection plan

The above numerical experiments provided the computing results of the objective value to validate the effectiveness and efficiency of the devised algorithm in solving a real-world instance, but they did not present the obtained UAV inspection plan. This subsection demonstrates the practical application of our approach in making real-world inspection plans.

To simulate the real-world instance as realistically as possible, we generated an instance with six UAVs, 20 monitoring sites, and eight charging stations, based on a realistic situation in which ① the monitoring sites are placed in an average manner within the construction area of the SZYB, ② the charging stations are distributed in corresponding construction areas to satisfy the
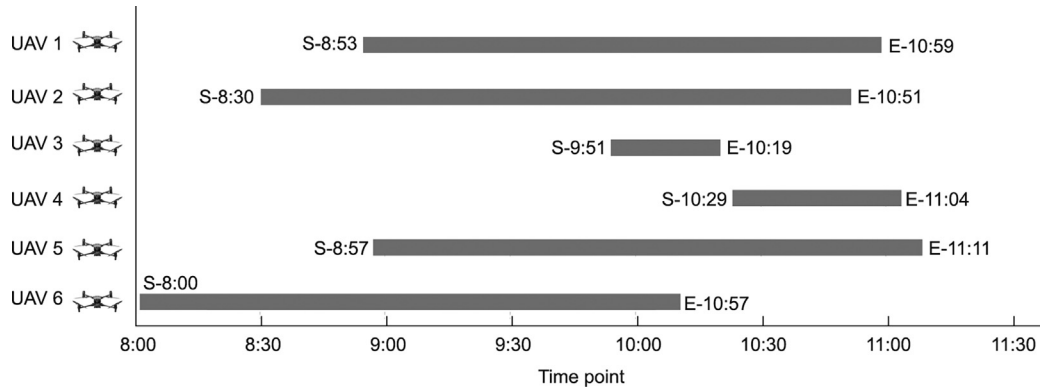
Fig. 12. Gantt chart of the inspection work. S: the time departing from the origination; E: the time completing all inspection tasks and arriving at the destination.

charging demand, and ③ each UAV begins its inspection tasks on one side of the SZYB and ends these tasks on the other side. On the basis of these requirements, a real-world instance is illustrated in Fig. S3 in Appendix A. Here, we needed to generate a practical inspection plan for a certain number of UAVs.

The inspection plan obtained using our approach is presented in Table 9, and the Gantt chart of the inspection plan is presented in Fig. 12. Because of space limitations, information on the charging decisions of the UAVs is omitted from the chart. The following insights were gained from the results for the real-world case. First, it was found that all of the UAVs, except for UAV 3 and UAV 4, continuously performed inspection tasks for a long time. UAV 3 and UAV 4 could be regarded as "emergency workers" dedicated to performing inspection tasks that may not be completed by other "busy" UAVs. Second, the time intervals between two consecutive inspection tasks of a UAV were usually shorter than 10 min but sometimes much longer than 10 min (e.g., 18 min between tasks 13-1 and 2-2). Except in a case of a long distance between two inspection tasks, the time was mainly spent on charging. All time intervals were shorter than 30 min, meaning that the UAVs tended to charge frequently instead of returning to a charging station when nearly depleted of power. The latter charging strategy would result in UAVs spending a long time waiting to fully charge, which would violate the time interval requirement.

8. Conclusions

This paper explored the UAV inspection routing and scheduling problem in the context of engineering project construction; an MILP model was formulated to optimize the total working time of UAVs completing a set of monitoring tasks. The devised model comprehensively considers the limitations of no-fly zones, interval windows, and the power of each UAV when developing UAV inspection routing and scheduling plans. A VNS-based metaheuristic was developed to solve the devised model efficiently. Numerical experiments were performed to validate the effectiveness of the devised model and algorithm. Finally, a case study of the SZYB project was conducted to derive practical insights for engineering managers that would enable them to optimize the efficiency of inspection works. The major contributions of the study are summarized as follows.

(1) From a modeling perspective, we comprehensively considered specific constraints in determining a UAV inspection plan using a devised MILP model—that is, no-fly zone limitations, rolling monitoring interval time window constraints, and power limitations. These specific constraints distinguish the devised model from typical models dedicated to the EVRP or EVRPTW. To the best of our knowledge, few papers have incorporated the above practical constraints in the context of engineering management into a mathematical model or have focused on the routing and scheduling of UAVs against the above background.

(2) From an algorithmic perspective, we developed a VNS-based metaheuristic to efficiently solve the devised model, as even a commercial solver struggles to find a feasible solution for this model in large-scale instances. A tailored neighborhood structure and initialization methods based on the specific features of the problem were developed. Extensive numerical experiments validated the efficiency of the devised algorithm for solving large-scale instances within 30 min.

(3) From a practical perspective, we gained several managerial insights from sensitivity experiments. For example, the suitable number of UAVs for performing different numbers of inspection tasks should be evaluated. Extensive investment in purchasing UAVs for inspections may not necessarily reduce the total working time; instead, it may increase unnecessary costs. A comparative experiment showed that an engineering manager purchasing UAVs within a limited budget should prioritize the velocity of the UAVs, followed by their power consumption per unit distance, and finally their battery power. Finally, it is best for UAVs—especially those conducting numerous inspection tasks—to charge frequently, as this reduces the time they have to wait to become fully charged.

This paper makes contributions to the inspection routing and scheduling optimization of UAVs in the context of engineering management; however, topics deserving of investigation still remain. As mentioned above, the optimal number of UAVs for different scales of inspection work should be further explored. In addition, current research has not fully addressed the uncertainty associated with drone inspection processes, such as weather conditions and changes in construction activities, which can significantly impact UAV energy consumption. Exploring and conducting in-depth research on how to perform better region clustering for monitoring points in order to reduce the scope of drone inspection is equally worth considering.

CRediT authorship contribution statement

Lu Zhen: Conceptualization, Investigation, Methodology, Writing-Original draft preparation, Writing-Reviewing and Editing, Supervision, Project administration, Funding acquisition. **Zhiyuan Yang:** Investigation, Methodology, Data curation, Software, Writing-Original draft preparation, Writing-Reviewing and Editing. **Gilbert Laporte:** Conceptualization, Investigation, Writing-Reviewing and Editing. **Wen Yi:** Investigation, Methodology,

Compliance with ethics guidelines

Lu Zhen, Zhiyuan Yang, Gilbert Laporte, Wen Yi, and Tianyi Fan declare that they have no conflict of interest or financial conflicts to disclose.

Appendix A. Supplementary data

Supplementary data to this article can be found online at https://doi.org/10.1016/j.eng.2023.10.014.

References

[1] Sajid M, Mittal H, Pare S, Prasad M. Routing and scheduling optimization for UAV assisted delivery system: a hybrid approach. Appl Soft Comput 2022;126:109225.

[2] Salama MR, Srinivas S. Collaborative truck multi-drone routing and scheduling problem: package delivery with flexible launch and recovery sites. Transp Res, Part E Logist Trans Rev 2022;164:102788.

[3] Qu X, Zeng Z, Wang K, Wang S. Replacing urban trucks via ground–air cooperation. Communications in Transportation Research 2022;2:100080.

[4] Manyam S, Sundar K, Casbeer D. Cooperative routing for an air-ground vehicle team-exact algorithm, transformation method, and heuristics. IEEE Trans Autom Sci Eng 2020;17(1):537–47.

[5] Sundar K, Venkatachalam S, Manyam S. Path planning for multiple heterogeneous unmanned vehicles with uncertain service times. In: Proceedings of 2017 International Conference on Unmanned Aircraft Systems (ICUAS); 2017 Jun 13-16; Miami, FL, USA. Piscataway: IEEE; 2017.

[6] Zheng Y, Du Y, Sheng W, Ling H. Collaborative human–UAV search and rescue for missing tourists in nature reserves. INFORMS Journal on Applied Analytics 2019;49(5):371–83.

[7] Li M, Zhen L, Wang S, Lv W, Qu X. Unmanned aerial vehicle scheduling problem for traffic monitoring. Comput Ind Eng 2018;122:15–23.

[8] Yi W, Wang H, Jin Y, Cao J. Integrated computer vision algorithms and drone scheduling. Commu in Transp Res 2021;1:100002.

[9] Du J, Weng F. Construction management and technology innovation for main projects of Quanzhou Bay Bridge. Front of Eng Manag 2021;8(1):151–5.

[10] Khan SI, Qadir Z, Munawar HS, Nayak SR, Budati AK, Verma KD, et al. UAVs path planning architecture for effective medical emergency response in future networks. Phys Commun 2021;47:101337.

[11] Chowdhury S, Shahvari O, Marufuzzaman M, Li X, Bian L. Drone routing and optimization for post-disaster inspection. Comput Ind Eng 2021;159:107495.

[12] Liu W, Zhang T, Huang S, Li K. A hybrid optimization framework for UAV reconnaissance mission planning. Comput Ind Eng 2022;173:108653.

[13] Shen L, Hou Y, Yang Q, Lv M, Dong J, Yang Z, et al. Synergistic path planning for ship-deployed multiple UAVs to monitor vessel pollution in ports. Transp Res Part D Transp Environ 2022;110:103415.

[14] Munishkin AA, Milutinović D, Casbeer DW. Min–max time efficient inspection of ground vehicles by a UAV team. Robot Auton Syst 2020;125:103370.

[15] Spencer B, Hoskere V, Narazaki Y. Advances in computer vision-based civil infrastructure inspection and monitoring. Engineering 2019;5(2):199–222.

[16] Perry BJ, Guo Y, Atadero R, Van de Lindt J. Streamlined bridge inspection system utilizing unmanned aerial vehicles (UAVs) and machine learning. Measurement 2020;164:108048.

[17] Hu J, Niu H, Carrasco J, Lennox B, Arvin F. Fault-tolerant cooperative navigation of networked UAV swarms for forest fire monitoring. Aerosp Sci Technol 2022;123:107494.

[18] Bailon-Ruiz R, Bit-Monnot A, Lacroix S. Real-time wildfire monitoring with a fleet of UAVs. Robot Auton Syst 2022;152:104071.

[19] Meng D, Xiao Y, Guo Z, Jolfaei A, Qin L, Lu X, et al. A data-driven intelligent planning model for UAVs routing networks in mobile Internet of Things. Comput Commun 2021;179:231–41.

[20] Xia Y, Batta R, Nagi R. Controlling a fleet of unmanned aerial vehicles to collect uncertain information in a threat environment. Oper Res 2017;65(3):674–92.

[21] Mbiadou Saleu R, Deroussi L, Feillet D, Grangeon N, Quilliot A. The parallel drone scheduling problem with multiple drones and vehicles. Eur J Oper Res 2022;300(2):571–89.

[22] Sacramento D, Pisinger D, Ropke S. An adaptive large neighborhood search metaheuristic for the vehicle routing problem with drones. Transp Res, Part C Emerg Technol 2019;102:289–315.

[23] Zhen L, Gao J, Tan Z, Wang S, Baldacci R. Branch-price-and-cut for trucks and drones cooperative delivery. IIE Trans 2022;55(3):271–87.

[24] Rajan S, Sundar K, Gautam N. Routing problem for unmanned aerial vehicle patrolling missions: a progressive hedging algorithm. Comput Oper Res 2022;142:105702.

[25] Xu C, Xu M, Yin C. Optimized multi-UAV cooperative path planning under the complex confrontation environment. Comput Commun 2020;162:196–203.

[26] Qin W, Shi Z, Li W, Li K, Zhang T, Wang R. Multiobjective routing optimization of mobile charging vehicles for UAV power supply guarantees. Comput Ind Eng 2021;162:107714.

[27] Hu M, Liu W, Lu J, Fu R, Peng K, Ma X, et al. On the joint design of routing and scheduling for vehicle-assisted multi-UAV inspection. Future Gener Comput Syst 2019;94:214–23.

[28] Zhen L, Li M, Laporte G, Wang W. A vehicle routing problem arising in unmanned aerial monitoring. Comput Oper Res 2019;105:1–11.

[29] Wang Y, Li Y, Yin F, Wang W, Sun H, Li J, et al. An intelligent UAV path planning optimization method for monitoring the risk of unattended offshore oil platforms. Process Saf Environ Prot 2022;160:13–24.

[30] Coelho B, Coelho V, Coelho I, Ochi L, Haghnazar K, Lima M, et al. A multi-objective green UAV routing problem. Comput Oper Res 2017;88:306–15.

[31] Moshref-Javadi M, Hemmati A, Winkenbach M. A truck and drones model for last-mile delivery: A mathematical model and heuristic approach. Appl Math Model 2020;80:290–318.

[32] Huang S, Huang Y, Blazquez C, Paredes-Belmar G. Application of the ant colony optimization in the resolution of the bridge inspection routing problem. Appl Soft Comput 2018;65:443–61.

[33] Zhen L, Wang B, Li M, Wang W, Huang L. Inspection routing problem for coal mine safety personnel in underground mines. Comput Ind Eng 2019;130:526–36.

[34] Jeong E, Seo J, Wacker J. UAV-aided bridge inspection protocol through machine learning with improved visibility images. Expert Syst Appl 2022;197:116791.

[35] Dji. The technology parameter of M300 RTK [Internet]. Shenzhen: Shenzhen Dajiang Innovation Technology Co., Ltd. © 2023 [cited 2023 Apr 1]. Available from: https://www.dji.com/cn/matrice-300/specs.

[36] Department of Transport of Guangdong Province. The new member of the cross-river channel group in the Greater Bay Area - the Shiziyang Passage project started the survey and design. Guangzhou: Guangdong Provincial Department of Transportation; 2021 Mar 3 [cited 2023 Apr 1]. Available from: http://td.gd.gov.cn/gkmlpt/content/3/3233/post_3233793.html#1479. [Chinese].